

Sensitive micromechanical displacement detection by scattering evanescent optical waves

Onur Basarir,^{1,3} Suraj Bramhavar,^{2,3} Gilberto Basilio-Sanchez,^{2,3} Theodore Morse,^{2,3} and Kamil L. Ekinci^{1,3,*}

¹Department of Mechanical Engineering, Boston University, Boston, Massachusetts 02215, USA

²Department of Electrical and Computer Engineering, Boston University, Boston, Massachusetts 02215, USA

³The Photonics Center, Boston University, Boston, Massachusetts 02215, USA

*Corresponding author: ekinci@bu.edu

Received February 24, 2010; revised April 20, 2010; accepted April 23, 2010;
posted May 5, 2010 (Doc. ID 124656); published May 19, 2010

We describe a simple approach to detect small mechanical displacements by scattering evanescent optical waves confined around an optical waveguide. Our experimental setup consists of a microcantilever brought into the proximity of a tapered optical fiber. The scattering of evanescent waves and hence the optical transmission through the tapered fiber is strongly dependent on the separation between the fiber and the microcantilever, allowing for sensitive detection of the small oscillations of the microcantilever. Our approach does not require a coherent laser source, yet it provides a displacement sensitivity of ~ 260 fm Hz^{-1/2} at a small power level of 38 μ W. It is suitable for scanning probe microscopy and could eventually be adapted to nanomechanical resonators. © 2010 Optical Society of America

OCIS codes: 120.7280, 120.4880, 120.5820.

Detecting the oscillations of micrometer- and nanometer-scale mechanical resonators [1,2] is an important component of many applications and fundamental measurements involving these devices. Most commonly, optical techniques are employed, providing very high sensitivities. These techniques can be implemented both on-chip [3–5] and off-chip [6–8] and have been demonstrated to work sensitively even for resonators with nanometer-scale linear dimensions. We can broadly classify optical techniques as either interferometric or noninterferometric. In interferometric detection, the resonator motion causes small detectable phase changes in the light reflected from its surface. Noninterferometric techniques, such as optical beam deflection [9] and knife-edge techniques [10], typically rely on changing or blocking the path of an optical beam, which is tightly focused onto the device. As such, both methods are often realized using coherent light sources.

In reality, noninterferometric techniques do not require coherent light sources, relaxing one of the stringent requirements of optical detection. Recently, for instance, an incoherent light source was used to demonstrate sensitive displacement detection in nanocantilever waveguides by relying on evanescent wave coupling [3]. In this Letter, we further these noninterferometric approaches: we demonstrate a near-field optical (evanescent wave)

technique, which is suitable for scanning probe microscopy and could eventually be adapted to nanomechanical resonators. Our technique exploits evanescent optical coupling between the weakly guided mode of an optical fiber taper and a microcantilever when the two are positioned in close proximity. The approach is sensitive enough to resolve the thermomechanical oscillations of the microcantilever and robust enough to spatially map out its first two resonant modes.

Our experimental configuration is shown in Figs. 1(a) and 1(b), consisting primarily of an optical fiber taper and a commercial tipless microcantilever, each being held in place by precision stages. The silicon microcantilever is approximately 230 μ m long, 38 μ m wide, and 7 μ m thick and is mounted on a small piezoelectric transducer for actuation. The optical microscope image in Fig. 1(c) shows the orientation of the microcantilever with respect to the fiber taper. The taper is formed by pulling a standard single-mode silica glass fiber with a core diameter of 9 μ m and an outer diameter of 125 μ m in a custom apparatus. This pulling apparatus simultaneously heats a portion of the fiber with a flame and pulls the fiber at opposite ends, creating a ~ 1 mm long tapered region with an outer diameter of ~ 1 μ m. Light from a broadband amplified spontaneous emission source is divided equally between a power monitor and the fiber

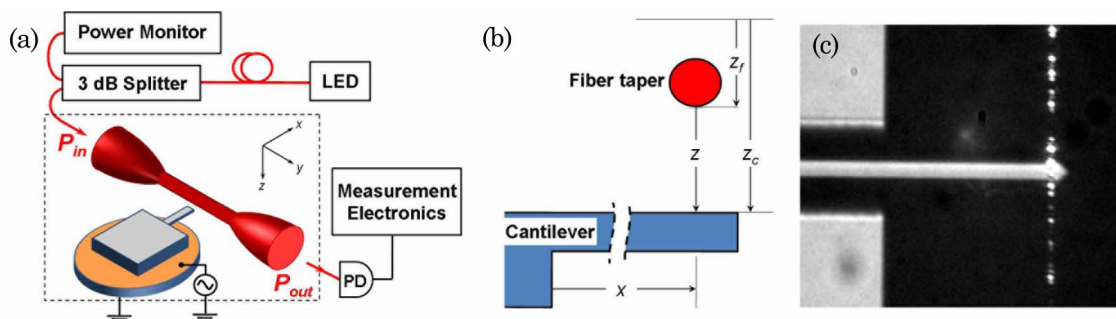


Fig. 1. (Color online) (a) Schematic of the experimental setup. (b) Cross-sectional view showing the coordinate system. (c) Microscope image of the fiber taper and microcantilever. Visible light is passed through the fiber taper in this image.

taper. In the experiments, a total input power of $125 \mu\text{W}$ at wavelengths ranging from 1400 to 1700 nm is sent through the fiber taper and onto a photodetector. The resulting power on the photodetector is $38 \mu\text{W}$ owing to the losses in the taper.

The optical modes in the fiber become weakly guided along the tapered section, with evanescent tails around. When the microcantilever comes sufficiently close to the fiber taper, these evanescent waves are coupled into the higher index Si and are lost [11]. The coupling and hence the optical power transmitted through the fiber taper is strongly dependent on the position of the microcantilever, i.e., the fiber taper-microcantilever separation. Given the taper diameter, we estimate the decay length of the evanescent field around the fiber taper to be $\sim 600 \text{ nm}$ [12]. We first study the transmission T through the fiber taper-microcantilever system by monitoring the transmitted dc optical power as a function of the vertical microcantilever position z_c [Fig. 1(b)]. The results from these measurements are shown in Fig. 2(a). The transmission is plotted as a function of the fiber taper-microcantilever gap z , where $z = z_c - z_f$ [Fig. 1(b)]. An attractive force F_a between the fiber taper and the microcantilever is expected to pull the fiber taper a small distance $\Delta z_f = F_a/\kappa_f$ toward the microcantilever as the microcantilever is stepped a distance Δz_c toward the fiber taper. Here, κ_f is the mechanical stiffness of the fiber taper. Both optical gradient forces [13,14] and van der Waals type forces [15] have been considered to obtain $F_a \sim 1 \text{ pN}$ for $z > 100 \text{ nm}$. A calculation based on measured taper dimensions and the theory of elasticity [16] yields $\kappa_f \approx 1 \text{ mN/m}$ (the resonance frequency of the fiber, in agreement with this κ_f value, is measured as $f_f \approx 420 \text{ Hz}$), and subsequently, $\Delta z_f \sim 1 \text{ nm}$. Thus we conclude that we are operating in a regime where $\Delta z \approx \Delta z_c$, except when the fiber taper and microcantilever are very close. We note that our thermal noise measurements and analysis below provide strong support for the above conclusion. Returning to Fig. 2(a), we observe a unity transmission when there is no coupling between the fiber taper and the microcantilever. The transmission starts to decrease monotonically as z is decreased. Finally, it drops to a small value once the fiber taper snaps to the microcantilever. A small hysteresis region [Fig. 2(a) inset] is typically observed in the transmission as the two are separated.

Next, we turn to the detection of small thermomechanical oscillations of the microcantilever by monitoring changes in the transmitted signal. A point close to the free end of the microcantilever is brought into the proximity of the fiber taper until a desired dc transmission is observed. This dc transmission value, which we call bias, is kept constant. Low-frequency drifts in the system, e.g., due to the stages, are nulled by using a computer-controlled digital feedback loop. With the feedback on, the high-frequency spectrum of the transmission is monitored by using a spectrum analyzer. The same measurement is repeated at multiple z values [symbols in Fig. 2(a)]. A representative thermal noise spectrum taken at $z \approx 0.58 \mu\text{m}$ [arrow in Fig. 2(a)] is displayed in the inset of Fig. 2(b). The resonance frequency and the quality factor of the fundamental mode are $f_1 \approx 158.7 \text{ kHz}$ and $Q_1 \approx 460$, respectively. The displacement calibration was done by using the equipartition

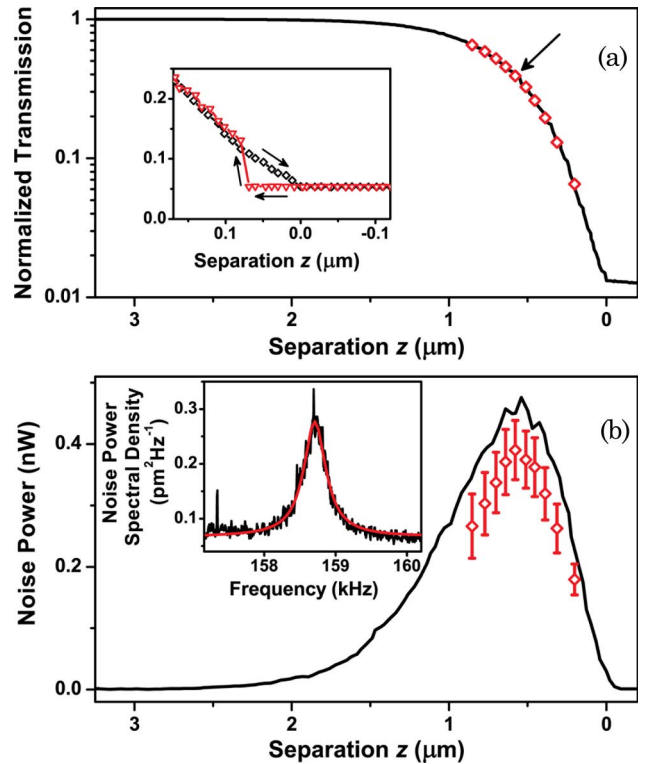


Fig. 2. (Color online) (a) Normalized optical transmission T as a function of the separation z (solid curve). Symbols correspond to z values at which thermal noise spectra are measured. The inset shows a typical hysteresis behavior obtained from approach and retract curves. (b) Detection of small oscillations using the transmission properties of the system in (a). The solid curve is calculated from Eq. (1) by using experimental parameters, and data shown by symbols are obtained from spectrum analyzer measurements. The inset shows the thermal noise power spectral density of the microcantilever in its fundamental mode. The solid curve is a fit to a Lorentzian line shape. The data are taken at $z \approx 580 \text{ nm}$.

theorem result, $\langle \delta z_c^2 \rangle = k_B \theta / \kappa_c$, where k_B is the Boltzmann constant, θ is the absolute temperature, and κ_c is the stiffness of the microcantilever mode. Given

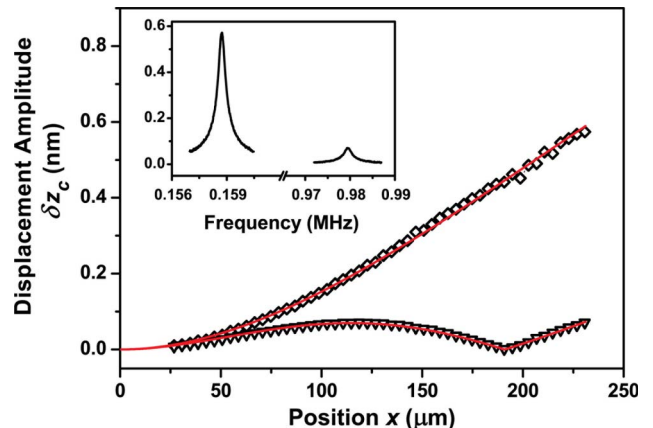


Fig. 3. (Color online) Displacement amplitudes in the first two out-of-plane modes of the microcantilever measured by positioning the fiber taper along the length of the microcantilever. Solid curves are fits obtained from theoretical calculations. The inset shows the resonance line shapes measured close to the free end of the microcantilever. For all the measurements, the dc component of P_{out} is $\sim 32 \mu\text{W}$.

the dimensions of the microcantilever, we obtain $\kappa_c \approx 30$ N/m, which results in an rms oscillation amplitude $\delta z_c \approx 11.2$ pm close to its free end.

We now turn to a more quantitative discussion of the displacement detection. If there are small changes in the gap as a function of time, the optical power P_{out} on the photodetector can be approximated as

$$P_{\text{out}}(t) \approx P_{\text{in}} \left[T + \left| \frac{\partial T}{\partial z} \right| \delta z(t) \right]. \quad (1)$$

The derivative is evaluated at the bias point; P_{in} is the dc input power. P_{out} has a dc background and a small time-dependent component. The derivative $|\partial T/\partial z|$ determines the displacement sensitivity. Small oscillations of both the microcantilever and the fiber taper with respective amplitudes $\delta z_c(t)$ and $\delta z_f(t)$ cause a modulation in T . However, they are at very different frequencies ($f_1 \approx 158.7$ kHz and $f_f \approx 420$ Hz), and both are sharply peaked. The derivative $|\partial T/\partial z|$ can be obtained by numerically differentiating the transmission versus z data of Fig. 2(a). Figure 2(b) shows the result of this differentiation multiplied by experimental parameters of $P_{\text{in}} \approx 38$ μ W and $\delta z_c \approx 11.2$ pm, as suggested in Eq. (1). The symbols in Fig. 2(b) represent the experimentally measured integrated noise power of microcantilever fluctuations at various bias points [see Fig. 2(a)]. The agreement between the curve obtained by using Eq. (1) and the experimental data suggests that the approximations and the analysis above are sound.

The displacement sensitivity in this measurement is determined by $|\partial T/\partial z|$ and the noise coming from the amplified spontaneous emission source. The maximum sensitivity is obtained at $z \approx 580$ nm. This maximum is achieved because, with increasing z , the evanescent coupling decreases while the transmitted power increases. Using the maximum value $|\partial T/\partial z| \approx 1.1$ μm^{-1} , we obtain a noise floor ~ 260 fmHz $^{-1/2}$ with 38 μ W input power (15 μ W incident on the photodetector).

To show the versatility of the approach, we map out the first two out-of-plane modes of the microcantilever. Prior to these measurements, we carefully calibrated the oscillation amplitude of the microcantilever by using a Michelson interferometer, while it was excited coherently by the piezo transducer. In Fig. 3, we display the rms oscillation amplitude as a function of position x along the microcantilever at its fundamental and first-harmonic resonances as measured by using the fiber taper setup. The data are obtained from swept frequency measurements [Fig. 3 inset] at various fiber positions x along the microcantilever. The resonance frequencies of the first two modes are $f_1 \approx 158.7$ kHz and $f_2 \approx 979.6$ kHz. The extracted quality factors are $Q_1 \approx 460$ and $Q_2 \approx 590$, consistent with air damping [17]. The gray

(red) curves in the plots are nonlinear least-square fits to the theoretical mode-shape functions for a cantilever beam [16]. Here, the clamping position is taken as an additional fitting parameter, since motion around the clamps is not detectable.

In summary, we have demonstrated a simple and sensitive noninterferometric displacement detection technique based on evanescent wave scattering. The technique does not require a coherent optical source and may find use in scanning probe microscopy and nanomechanical displacement detection.

We acknowledge support from the U.S. National Science Foundation (NSF) through grant ECCS-0643178. O. Basarir was supported by a BU Photonics Center fellowship. We thank O. Ozsun for help with optical interferometry and A. Vandelay for discussions.

References

1. K. L. Ekinici and M. L. Roukes, *Rev. Sci. Instrum.* **76**, 061101 (2005).
2. N. V. Lavrik, M. J. Sepaniak, and P. G. Datskos, *Rev. Sci. Instrum.* **75**, 2229 (2004).
3. M. Li, W. H. P. Pernice, and H. X. Tang, *Nat. Nanotechnol.* **4**, 377 (2009).
4. I. D. Vlamincx, J. Roels, D. Taillaert, D. V. Thourhout, R. Baets, L. Lagae, and G. Borghs, *Appl. Phys. Lett.* **90**, 233116 (2007).
5. G. Anetsberger, O. Arcizet, Q. P. Unterreithmeier, R. Riviere, A. Schliesser, E. M. Weig, J. P. Kotthaus, and T. J. Kippenberg, *Nat. Phys.* **5**, 909 (2009).
6. Q. P. Unterreithmeier, S. Manus, and J. P. Kotthaus, *Appl. Phys. Lett.* **94**, 263104 (2009).
7. N. Liu, F. Giesen, M. Belov, J. Losby, J. Moroz, A. E. Fraser, G. McKinnon, T. J. Clement, V. Sauer, W. K. Hiebert, and M. R. Freeman, *Nat. Nanotech.* **3**, 715 (2008).
8. S. S. Verbridge, H. G. Craighead, and J. M. Parpia, *Appl. Phys. Lett.* **92**, 013112 (2008).
9. G. Meyer and N. M. Amer, *Appl. Phys. Lett.* **53**, 1045 (1988).
10. D. Karabacak, T. Kouh, C. C. Huang, and K. L. Ekinici, *Appl. Phys. Lett.* **88**, 193122 (2006).
11. D. M. Karabacak, K. L. Ekinici, C. H. Gan, G. J. Gbur, M. S. Ünlü, S. B. Ippolito, B. B. Goldberg, and P. S. Carney, *Opt. Lett.* **32**, 1881 (2007).
12. B. E. Little, J.-P. Laine, and H. A. Haus, *J. Lightwave Technol.* **17**, 704 (1999).
13. M. Eichenfield, C. P. Michael, R. Perahia, and O. Painter, *Nat. Photon.* **1**, 416 (2007).
14. M. L. Povinelli, M. Loncar, M. Ibanescu, E. J. Smythe, S. G. Johnson, F. Capasso, and J. D. Joannopoulos, *Opt. Lett.* **30**, 3042 (2005).
15. J. N. Israelachvili, *Intermolecular and Surface Forces*, 2nd ed. (Academic, 1992).
16. A. N. Cleland, *Foundations of Nanomechanics*, 1st ed. (Springer, 2002).
17. D. M. Karabacak, V. Yakhot, and K. L. Ekinici, *Phys. Rev. Lett.* **98**, 254505 (2007).